Automatic Detection of Myocardial Perfusion Defects using Object-based Myocardium Segmentation

Teodora Chitiboi[1,2], Anja Hennemuth[1], Lennart Tautz[1], Paul Stolzmann[3], Olivio F Donati[3], Lars Linsen[2], Horst K Hahn[1,2]

[1] Fraunhofer MEVIS Institute for Medical Image Computing, Bremen, Germany
[2] Jacobs University Bremen, Germany
[3] Institute for Diagnostic and Interventional Radiology, University Hospital Zurich, Switzerland

Abstract

Determining the relevance of coronary artery pathologies is a major task in diagnosis and therapy planning for coronary heart disease. Magnetic resonance (MR) perfusion imaging provides non-invasive means to assess the influence of artery stenosis on the myocardial perfusion. The overall goal of the presented approach is to enable a fully automatic data analysis that supports both the conventional AHA model perfusion quantification and a voxel-based segmentation of suspicious regions in the heart muscle. To this end, an automatic pipeline for detecting and segmenting perfusion defects was developed and evaluated. The myocardium is segmented using an object-based image analysis approach, which then forms the basis for the perfusion parameter calculation and detection of underperfused regions. The approach has been applied to six datasets of patients with known multivessel coronary heart disease. Results show a good agreement with findings from MR delayed enhancement examination and conventional coronary angiography.

1. Introduction

Alongside with cancer and stroke, coronary heart disease is one of the most common diseases in the aging society. Pathological changes of the vessel walls, so-called vessel plaque, can cause narrowings of the vessel lumen. If this hinders the blood flow such that the heart muscle (myocardium) cannot be supplied with sufficient oxygen, the muscle tissue degenerates. Cardiac perfusion MRI provides the means for non-invasive detection of underperfused myocardial tissue. The analysis of image sequences that show the wash-in and wash-out of a contrast agent in the bloodpool and the myocardium is however challenging because of the breathing and contractile motion of the heart and the strong intensity changes in the image compartments.

An overview of existing approaches for image preprocessing and parameter extraction from time-intensity curves is given by Gupta et al. [1]. In the literature, this is either achieved through the identification of corresponding regions in every time frame using manual or automatic segmentation methods [2–4] or through time frame alignment followed by segmentation of the myocardium in one image that represents the corrected sequence [5, 6]. The first concept only enables the conventional AHA-model-based analysis of averaged perfusion curves, whereas the latter approach computes parameter maps that enable the segmentation of hypoperfused regions and is therefore adopted here. Accurate information about the location, size and degree of a hypoperfusion are of clinical interest, and there are some approaches to segment suspicious regions based on the inspection of voxel intensity curves. These use different classification approaches such as factor analysis, fuzzy k-means [7] and support vector machines [8], but do not incorporate spatial constraints given for the location of infarctions relative to the myocardial wall.

In this work we present and evaluate a method combination for the automatic detection of underperfused myocardial tissue regions. One novel step that facilitates our goal is the automatic object-based image analysis (OBIA) method for segmenting the myocardium in temporal maximum-intensity projection (MIP) images. The presented pipeline combines unspecific registration and segmentation approaches with anatomical and disease-specific knowledge, with a view to enable applicability to image data acquired with different scanners and settings.

2. Overview and setup

The proposed processing pipeline consists of three steps, namely initialization and motion correction, the detection of the myocardium and the analysis of the local myocardial perfusion, as shown in Fig. 1.

In the setup phase we used the intensity variation

$\sigma^2_{\max}(\mathbf{x})$ per pixel $\mathbf{x}$ during a time interval T, which represents the average time from the venous contrast agent injection to tissue enhancement, in order to suppress regions with constant high intensities. We then determine the left and right ventricular bloodpools by clustering pixel areas using $\sigma^2_{\max}(\mathbf{x})$. Their corresponding time-intensity curves are used to determine the reference time point t_{ref} with similar intensities for the two clusters, used for the subsequent motion correction. The correction method applied uses the local phase, which represents image features such as edges and lines but is invariant to their magnitude [9]. The multiscale implementation enables the correction of stronger displacements as induced by breathing as well as local deformations caused by contractile motion.

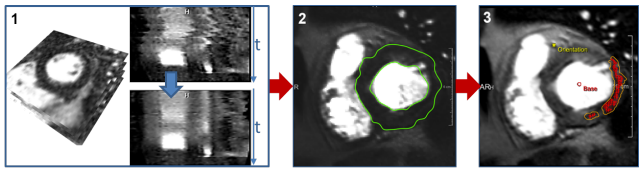

Figure 1: Processing steps for the automatic perfusion defect detection: (1) Motion correction; (2) Myocardium detection; (3) Analysis of local myocardial perfusion.

3. Object-based segmentation

The detection of the myocardial contours is performed on the temporal MIP (Fig. 2-1), after the preceding registration step described in Section 2. This allows a clear delineation of the myocardium (dark ring) as well as the left and right ventricular bloodpools (bright).

Segmentation is performed using an OBIA approach based on the generic concept proposed by Homeyer et al. [10]. In this setting, the atomic semantic structures used to analyze images are not individual pixels but pixel regions called objects, which are described by a set of properties regarding shape, orientation, intensity statistics and relative position. The objects are defined by an initial image partition obtained using a k-means clustering method called SLIC [11], which compromises between an object's homogeneity and compactness. Starting with this oversegmented image (Fig. 2-2), we successively merge pairs of adjacent objects in a heuristic fashion using their intensity and shape properties to obtain the left ventricle (LV) bloodpool and myocardium. We assume that the bloodpool is compact, elliptic and includes the papillary muscles, while the myocardium is at most 3cm thick.

First, a seed point s is determined close to the center of the LV in each slice of the MIP image I using the Hough transform [12]. Then, the bloodpool is roughly estimated by region growing on the object level starting from s. Neighboring objects are added as long as their median intensity value is brighter than an adaptive threshold $t = f(I(s))$, where f was empirically determined. Next,

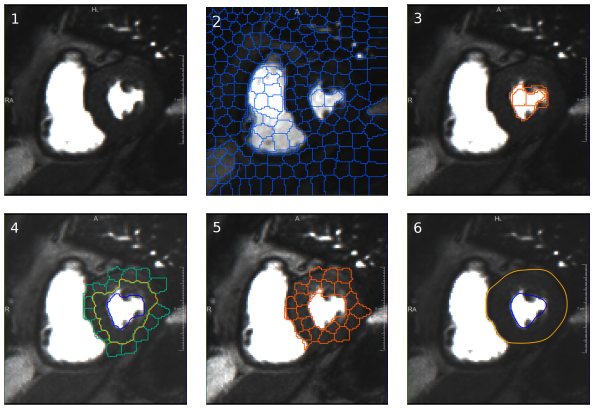

Figure 2: (1)Temporal MIP; (2)Initial objects; (3)Bloodpool after region growing and ellipse fitting; (4)Initial myocardium estimation (yellow) and further objects considered (green); (5)Myocardium objects; (6)Active contours result.

a best fitting ellipse is computed using principal component analysis (PCA) and all neighboring objects more than 50% covered are also merged to include the papillary muscles partially surrounded by blood. To obtain a compact segmentation, small neighboring objects are added to minimize the contour length of the resulting region (Fig. 2-3).

Next, the myocardium is initialized by merging the first ring of objects neighboring the bloodpool (Fig. 2-4 in yellow). For this set of initial myocardium objects we compute the average lower and upper quartiles $\bar{l}$ and $\bar{u}$ and their standard deviations dl and du. Further neighboring objects p' with similar lower and upper quartiles l' and u' are considered in a subsequent region growing step iff. $\bar{l} - 2dl < l'$ and $u' < \bar{u} + 2du$ (Fig. 2-4 green). An object p' neighboring a myocardium object p is also classified as part of the myocardium iff. $|avg(p) - avg(p')| < 0.004$ where avg represents the average intensity of the object normalized to $[0, 1]$. This local measure accounts for significant intensity differences that can appear in certain areas of the myocardium. Then, the shape of the joint myocardium-bloodpool mask is similarly optimized using ellipse overlap and a minimal contour constraint(Figure 2-5).

The coarse result obtained by object-based segmentation is locally refined using the active contour (AC) algorithm introduced by Kass et al. [13]. Without an accurate initialization the AC would not directly converge to the desired contour because of the very low contrast, so we use a fixed number of iterations to smooth the result while following any clearly visible edges (Fig. 2-6).

4. Intensity curve analysis

The relationship between measured intensities and contrast agent concentration is non-linear and depends strongly on the contrast agent, its local concentration, field inhomogeneities, etc. [14]. Thus, there are no standardized values which could be used for a threshold-based detection of perfusion defects based on quantitative parameters.

Our approach to perfusion defect detection is based on similar assumptions applied for the segmentation of necrotic or fibrotic tissue from delayed enhancement MRI [15]. The segmentation algorithm is based on a Gaussian-mixture histogram analysis to determine suitable thresholds for quantitative perfusion parameters such as myocardial bloodflow (MBF) and can be used in conjunction with descriptive parameters such as the upslope of the time-intensity curve. First, suitable seedpoints are detected in the subendocardial part of the myocardium applying the threshold derived from the Gaussian-mixture histogram analysis. These seedpoints are then used as input for the watershed transform by Hahn and Peitgen [16] to determine the underperfused regions.

For the calculation of the quantitative parameters with the singular value decomposition (SVD) implementation as proposed by Ostergaard et al. [17], the arterial input function (AIF) is required. This was set to the contrast agent's first pass through the left ventricle, which is represented by the gamma variate fit to the time-intensity curve of the left ventricular bloodpool.

5. Evaluation

5.1. Data

The described myocardium segmentation algorithm was applied to nine MRI perfusion datasets of patients with coronary artery disease. The datasets were acquired with a 1.5T Philips Intera scanner after an intravenous injection of gadobutrol (Gadovist 1.0; Bayer Schering Pharma). Contrast media was dosed at 0.1mmol/kg of body weight at an injection rate of 5ml/s, followed by a 40ml saline flush. K-t sensitivity encoding perfusion CMR imaging was combined with a saturation recovery gradient-echo pulse sequence. Three to four slices were acquired with 10mm thickness and in-plane resolution of $1.25 \times 1.25\text{mm}^2$ after contrast agent injection over 40 to 65 consecutive heartbeats. These sequences illustrate the contrast agent's first pass through the myocardium. For six of the patients, the location of underperfused myocardial regions was determined by additional delayed enhancement MRI examinations which were manually segmented, as well as coronary angiographies. These datasets were further considered for the detection of perfusion defects.

5.2. Results

In order to assess the accuracy of the automatic myocardium segmentation we have considered two manual segmentations $M1$ and $M2$ as references for the automatic result A. The dice score (Dice) and the average and maximum symmetrical distance in mm (AvgD and MaxD) were computed for each pair of masks and summarized in Table 1. The large variability between the two reference segmentations is due to the low signal-to-noise ratio and poor contrast. Although the automatic segmentation performs slightly worse than a manual one, the average offset between an automatically generated and a manual contour is only slightly larger than between two references.

	Dice	STD	AvgD	STD	MaxD	STD
M1, M2	0.84	0.08	0.68	0.57	6.38	3.53
M1, A	0.73	0.06	1.34	0.59	11.04	3.39
M2, A	0.71	0.08	1.35	0.65	10.46	4.34

Table 1: Evaluating myocardium segmentation accuracy.

The method described in Section 4 has been successfully applied to the six datasets of patients with known perfusion defects. The segmented underperfused regions were visually compared with the corresponding delayed enhancement image data, as shown in Fig. 3 for a patient with known stenoses $> 75\%$ in the LAD and LCX arteries. The segmented perfusion defect includes the delayed enhancement region and corresponds to the known stenosis position. However, the accuracy of perfusion defects detection is difficult to quantify because the perfusion and delayed enhancement images usually differ in resolution, breathing phase and most importantly heart phase.

After resampling and manual registration using landmarks we visually compared the manual segmentation of the delayed enhancement images with the automatically segmented perfusion defects. Each individual afflicted region marked in the delayed enhancement was labeled as detected, partially detected or missed, as shown in Fig. 4. If a region was almost completely covered by the perfusion result up to a difference in the heart phase, it was labeled as detected. Out of a total of 21 individual regions highlighted in the delayed enhancement data, 14 were detected, 2 were partially detected and 5 were missed. Out of the missed regions, 4 were very small with an area $< 30\text{mm}^2$. Considering the total area of the delayed enhancement regions, we have reached a detection rate of 75.5%.

5.3. Discussion

The segmentation of the MIP images avoided the inclusions of myocardial regions for which misregistration would have led to the inclusion of bloodpool voxels into the intensity course analysis. Considering the large variability of manual delineations that reflects the difficulty of the segmentation task, our automatic results look very promising. However, some typical segmentation errors may occur such as inclusion of right ventricular myocardium or fat tissue, which we plan to improve.

The segmented underperfused areas are on average 2-3 times larger than the necrotic tissue detected in the delayed enhancement, in agreement with the likely scenario that a larger surrounding portion of the myocardium is af-

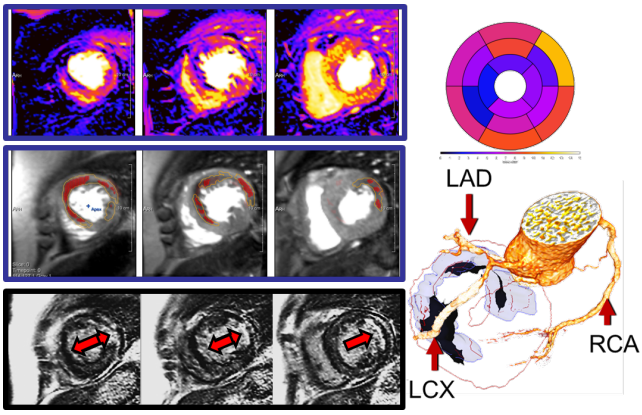

Figure 3: Top: MBF parameter images and AHA segment analysis after motion correction. Middle: Temp. MIP, initial markers (red) and perfusion defect segmentation (yellow). Bottom: delayed enhancement. Right: 3D visualization of diseased vessel branches, delayed enhancement segmentation (black), perfusion segmentation (blue) and myocardium (red).

fected by the reduced blood supply. A major limitation of the presented evaluation is the missing information about the relevance of the reported stenoses. It is thus not possible to accurately assess the segmentation quality in regions that do not exhibit delayed enhancement.

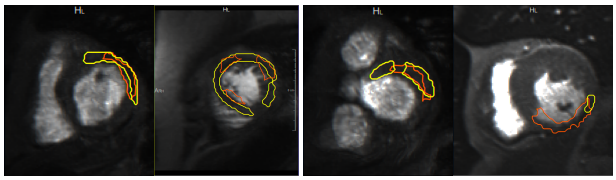

(a) Detected (b) Diff. phase (c) Partially (d) Missed

Figure 4: Sample results: delayed enhancement reference(orange) and perfusion segmentation (yellow).

6. Conclusions

We have presented and tested a myocardium segmentation algorithm that can be used in a larger pipeline for the detection of suspicious regions in perfusion data. The comparison with findings from other modalities showed a good correlation with our results. The clear delineation of the underperfused region is very promising and indicates the potential for a region detection, which allows a better inspection of extent and transmurality of perfusion defects. In combination with the coronary artery tree, the detection of the coronary arteries provide a promising non-invasive means for the assessment of coronary stenosis relevance. In order to evaluate the identification of underperfused viable tissue, which is not identifiable with delayed enhancement MRI, future work will use additional pressure wire measurements to improve the evaluation of the benefit provided by the presented methods.

References

[1] Gupta V, Kirisli H, Hendriks E, van der Geest R, van de Giessen M, Niessen W, Reiber J, Lelieveldt B. Cardiac MR perfusion image processing techniques: a survey. Med Image Anal May 2012;16(4):767–785.

[2] Spreeuwers L, Breeuwer M. Automatic Detection of Myocardial Boundaries in MR Cardio Perfusion Images. In MICCAI. 2001; 1228–1231.

[3] Santarelli M, Positano V, Michelassi C, Lombardi M, Landini L. Automated Cardiac MR Image Segmentation: Theory and Measurement Evaluation. Med Eng Phys Mar 2003;25(2):149–159.

[4] Horkaew P. Analysis of CMR Perfusion Imaging based on Statistical Appearance Models. In KST. 2010; 6–11.

[5] Gupta V, Hendriks E, Milles J, van der Geest RJ, Jerosch-Herold M, Reiber J, Lelieveldt B. Fully automatic registration and segmentation of first-pass myocardial perfusion mr image sequences. Acad Radiol 2010;17:1375–1385.

[6] Weng A, Ritter C, Lotz J, Beer M, Hahn D, Koestler H. Automatic Postprocessing for the Assessment of Quantitative Human Myocardial Perfusion using MRI. Eur Radiol Jun 2010;20(6):1356–1365.

[7] Di Bella E, Sitek A. Time Curve Analysis Techniques for Dynamic Contrast MRI Studies. In IPMI. 2001; 211–217.

[8] Hansen M, Ólafsdóttir H, Sjöstrand K, Erbou S, Stegmann M, Larsson H, Larsen R. Ischemic segment detection using the support vector domain description. SPIE 2007; 6512:65120F.

[9] Tautz L, Hennemuth A, Andersson M, Seeger A, Knutsson H, Friman O. Phase-based Non-rigid Registration of Myocardial Perfusion MR Image Sequences. In IEEE ISBI. 2010; 516–519.

[10] Homeyer A, Schwier M, Hahn H. A Generic Concept for Object-based Image Analysis. In VISAPP. 2010; 530–533.

[11] Achanta R, Shaji A, Smith K, Lucchi A, Fua P, Süsstrunk S. Slic superpixels. EPFL Tech Rep 2010;149300.

[12] Yip R, Tam P, Leung D. Modification of hough transform for circles and ellipses detection using a 2-dimensional array. Pattern Rec 1992;25(9):1007–1022.

[13] Kass M, Witkin A, Terzopoulos D. Snakes: Active Contour models. IJCV 1988;1(4):321–331.

[14] Jerosch-Herold M. Quantification of Myocardial Perfusion by Cardiovascular Magnetic Resonance. JCMR 2010; 12(57):1–16.

[15] Hennemuth A, Friman O, Huellebrand M, Peitgen HO. Mixture-model-based Segmentation of Myocardial Delayed Enhancement MRI. In STACOM. 2012; 87–96.

[16] Hahn H, Peitgen H. IWT – Interactive Watershed Transform: A hierarchical method for efficient interactive and automated segmentation of multidimensional grayscale images. In SPIE, volume 5032. SPIE, 2003; 643–653.

[17] Ostergaard L, Weisskoff R, Chesler D, Gyldensted C, Rosen B. High resolution measurement of cerebral blood flow using intravascular tracer bolus passages. Part I: Mathematical approach and statistical analysis. Magn Reson Med 1996; 36(5):715–725.